International Journal of Nanomedicine

Dovepress
open access to scientific and medical research

Open Access Full Text Article

ORIGINAL RESEARCH

Preparation of *Pueraria lobata* Root-Derived Exosome-Like Nanovesicles and Evaluation of Their Effects on Mitigating Alcoholic Intoxication and Promoting Alcohol Metabolism in Mice

Wenjin Zhang[1], Qiang Song[1], Xiaofei Bi[1], Wei Cui[1], Chengmei Fang[1], Jianya Gao[1], Jinan Li[1], Xiang Wang[1], Kai Qu[1], Xian Qin[1], Xuan An[2,3], Cheng Zhang[1,3], Xianxiang Zhang[1,3], Fang Yan[4], Guicheng Wu[1–3]

[1]Chongqing Municipality Clinical Research Center for Endocrinology and Metabolic Diseases, Chongqing University Three Gorges Hospital, Chongqing, People's Republic of China; [2]Department of Hepatology, Chongqing University Three Gorges Hospital, Chongqing, People's Republic of China; [3]School of Medicine, Chongqing University, Chongqing, People's Republic of China; [4]Geriatric Diseases Institute of Chengdu, Department of Geriatrics, Chengdu Fifth People's Hospital, Chengdu, People's Republic of China

Correspondence: Guicheng Wu, Chongqing University Three Gorges Hospital, Xincheng Road 165#, Wanzhou District, Chongqing, 404000, People's Republic of China, Tel +(86) 58103079, Fax +86 23 581045783, Email wuguicheng@cqu.edu.cn; Fang Yan, Geriatric Diseases Institute of Chengdu, Department of Geriatrics, Chengdu Fifth People's Hospital, Mashi Street 33#, Wenjiang District, Chengdu, 611130, People's Republic of China, Tel/Fax +86 28 82661127, Email fangyan@cdutcm.edu.cn

Purpose: *Pueraria lobata (P. lobata)*, a dual-purpose food and medicine, displays limited efficacy in alcohol detoxification and liver protection, with previous research primarily focused on puerarin in its dried roots. In this study, we investigated the potential effects and mechanisms of fresh *P. lobata* root-derived exosome-like nanovesicles (P-ELNs) for mitigating alcoholic intoxication, promoting alcohol metabolism effects and protecting the liver in C57BL/6J mice.

Methods: We isolated P-ELNs from fresh *P. lobata* root using differential centrifugation and characterized them via transmission electron microscopy, nanoscale particle sizing, ζ potential analysis, and biochemical assays. In Acute Alcoholism (AAI) mice pre-treated with P-ELNs, we evaluated their effects on the timing and duration of the loss of the righting reflex (LORR), liver alcohol metabolism enzymes activity, liver and serum alcohol content, and ferroptosis-related markers.

Results: P-ELNs, enriched in proteins, lipids, and small RNAs, exhibited an ideal size (150.7 ± 82.8 nm) and negative surface charge (−31 mV). Pre-treatment with 10 mg/(kg.bw) P-ELNs in both male and female mice significantly prolonged ebriety time, shortened sobriety time, enhanced acetaldehyde dehydrogenase (ALDH) activity while concurrently inhibited alcohol dehydrogenase (ADH) activity, and reduced alcohol content in the liver and serum. Notably, P-ELNs demonstrated more efficacy compared to P-ELNs supernatant fluid (abundant puerarin content), suggesting alternative active components beyond puerarin. Additionally, P-ELNs prevented ferroptosis by inhibiting the reduction of glutathione peroxidase 4 (GPX4) and reduced glutathione (GSH), and suppressing acyl-CoA synthetase long-chain family member 4 (ACSL4) elevation, thereby mitigating pathological liver lipid accumulation.

Conclusion: P-ELNs exhibit distinct exosomal characteristics and effectively alleviate alcoholic intoxication, improve alcohol metabolism, suppress ferroptosis, and protect the liver from alcoholic injury. Consequently, P-ELNs hold promise as a therapeutic agent for detoxification, sobriety promotion, and prevention of alcoholic liver injury.

Keywords: *Pueraria lobata* root-derived exosome-like nanovesicles, acute alcoholism, loss of the righting reflex, ethanol metabolism, ferroptosis

Introduction

The global burden of alcohol dependence and intoxication poses a significant public health challenge. As per World Health Organization (WHO) data from 2018, alcohol poisoning alone accounts for a staggering 18.57 million Disability-Adjusted Life

Received: 2 February 2024
Accepted: 22 May 2024
Published: 27 May 2024

Years (DALYs) lost.[1] Furthermore, projections suggest an upward trend in average adult alcohol consumption, from 5.9 liters in the 1990s to a projected 7.6 liters by 2030,[2] driven primarily by rising consumption in Asia and Africa.[3] Excessive alcohol exposure can lead to acute intoxication, characterized by temporary central nervous system dysfunction and variable organ damage. The liver is particularly vulnerable, with early manifestations often including alcoholic fatty liver disease. If untreated, this condition can progress to alcoholic hepatitis, liver fibrosis, and ultimately cirrhosis, culminating in liver failure.[4,5] Current treatment options for hangovers and alcohol metabolism remain limited. Notably, existing medications like opioids, benzodiazepines, and barbiturates carry significant risks, including addiction potential and residual effects.[6,7] Therefore, the development of novel, non-harmful dietary drugs for alcohol detoxification and liver protection is of paramount importance.

Recent advancements in plant biology have revealed the widespread secretion of extracellular vesicles (EVs) by plant cells. These EVs, ranging from 80 to 300 nm in diameter, are intricate nano-carriers encapsulating a diverse repertoire of bioactive molecules. Their remarkable antioxidative, anti-inflammatory, and anti-tumor properties have attracted significant attention, along with their crucial roles in intercellular communication.[8,9] To address the absence of uniform markers for plant-derived EVs, the International Society for Extracellular Vesicles revised its nomenclature in 2018, designating them as exosome-like nanovesicles (ELNs) or vesicle-like nanoparticles (VLNs).[10] Notably, these plant-derived ELNs exhibit promising potential in liver protection beyond their established biological activities. Emerging research suggests that ELNs isolated from microvesicles, enriched with bioactive compounds, can modulate diverse biological processes in the liver and other organs.[11] In this respect, *Ginger*-derived nanoparticles (GDNs) have demonstrated efficacy in protecting mice from alcohol-induced liver damage.[12] Similarly, pre-treatment with *Shiitake Mushroom*-derived exosome-like nanoparticles (S-ELNs) was found to confer protection against acute liver injury induced by D-galactosamine (GalN) and lipopolysaccharides (LPS) in murine models.[13] Moreover, *Pomegranate*-derived exosome-like nanovesicles (P-NVs) have been shown to mitigate intestinal leakage and liver damage associated with alcohol consumption.[14] In a noteworthy study, oral administration of *Oat* nanoparticles (oatN) prevented alcohol-induced activation of inflammatory signaling pathways in the brain, consequently enhancing memory function in mice.[15] However, the potential of *Pueraria lobata (P. lobata)* root-derived exosome-like nanoparticles (P-ELNs) in anti-Intoxication, alcohol metabolism-promoting effects and liver protection remains relatively unexplored.

The root and flower of the *P. lobata* plant, as mentioned in traditional medical texts such as "Qianjin Fang" for their reputed hangover relief properties, are recognized for their extracts abundant in flavonoids and isoflavones, with puerarin being the primary active component.[16,17] While *P. lobata* serves a dual purpose as both food and medicine, demonstrating effects in alcohol detoxification and liver protection, its effectiveness is directly proportional to the dosage, leading to suboptimal utilization.[18] This may be attributed to the potential loss of active components during traditional processing methods, with existing research primarily focusing on the puerarin content found in the root's dry powder. In our study, we refine extraction methods from previous literature[19–21] to produce high-concentration P-ELNs from *P. lobata* roots. These are then applied in an acute alcohol intoxication mice model to explore specific therapeutic effects and the underlying mechanisms. Given that the liver is the primary site of alcohol metabolism, it is subject to complex pathogenic mechanisms from alcohol exposure, prominently involving oxidative stress, inflammation, and hepatocyte death.[5]

Hepatocytes, characterized by an abundance of mitochondria, are highly susceptible to mitochondrial-linked programmed cell death (PCD) pathways, including apoptosis, ferroptosis, autophagy, and pyroptosis, following exposure to alcohol. Previous studies have demonstrated that alcohol exposure induces alterations in distinct biomarkers associated with ferroptosis.[22,23] Specifically, long-term ethanol consumption in male mice triggers ferroptosis, as evidenced by dysregulated ferroptosis-related gene expression, elevated lipid peroxidation, and intracellular iron accumulation in the liver.[24] Furthermore, studies have demonstrated the protective effects of ferroptosis inhibitors, such as ferrostatin-1, in mitigating alcohol-induced liver damage in female mice on an ethanol diet.[25] Additionally, an iron-deficient diet has been shown to attenuate the decline of glutathione peroxidase 4 (GPX4) and alleviate alcohol-induced liver injury by utilizing reduced glutathione (GSH) to detoxify malondialdehyde (MDA).[26] Despite these advancements, the potential role of plant exosomes in mediating ferroptosis during alcohol-induced liver damage remains uninvestigated, presenting a promising avenue for further research.

This study sought to examine the distinct therapeutic effects of P-ELNs in mice subjected to alcohol exposure while also delving into the potential involvement of ferroptosis mechanisms. Our investigation into P-ELNs not only enhances comprehension regarding plant exosomes but also holds the potential to propel advancements in research related to

alcohol detoxification and liver protection. This, in turn, contributes to the enhancement of therapeutic options in this domain for the improvement of human health and overall welfare.

Materials and Methods

Separation and Identification of P-ELNs

P. lobata was provided and identified by Chief pharmacist Boqun Li, Chongqing Technical Innovation Center for Quality Evaluation and Identification of Authentic Medicinal Herbs, in accordance with the standards set by the Chinese Pharmacopoeia. It is currently stored at the Pharmacy of Traditional Chinese Medicine, Chongqing University Three Gorges Hospital (No. 20200804GeGen).

Fresh *P. lobata* roots, is annually collected and meticulously selected from the Three Gorges Reservoir Area in China, specifically during the period between November and March, underwent a thorough cleansing process using deionized water followed by surface drying for preservation. Approximately 200 g of these fresh roots were finely cut into fragments smaller than 1 centimeter and pulverized using a grinding machine through 1 to 3 cycles until achieving a texture resembling fluffy meat. The ratio of fresh *P. lobata* to crushed *P. lobata* ranges from 1:0.9 to 1. Following this, 400 mL of 4°C pre-chilled PBS buffer was added at a ratio of 1:1.5–2 relative to the weight of the *P. lobata* roots material (g). The resulting mixture was securely sealed with plastic wrap and incubated overnight at 4°C on a shaker set to a low, uniform speed. This incubation process aimed to maximize the release of P-ELNs from the fresh *P. lobata* roots tissue into the PBS buffer. After the overnight incubation, large particles and impurities, such as remnants of the *P. lobata* roots, were eliminated using dual layers of medical gauze, and the *P. lobata* roots PBS buffer was collected. This buffer then underwent centrifugation in a high-speed refrigerated centrifuge (Allegra 64R, Beckman Coulter, US) at 2000 ×*g* for 30 minutes, followed by 10,000 ×*g* for 60 minutes. The resulting supernatant was further filtered using a 0.22 μm filter (SLGPR33RB, Millipore, Germany). Subsequently, the filtered supernatant was placed in an ultracentrifuge (Optima MAX-XP, Beckman Coulter, US) and centrifuged at 150,000 ×*g* for 120 minutes. At this stage, the precipitated particles obtained were identified as P-ELNs, and the supernatant above the precipitate was termed the *P. lobata* root-derived exosome-like nanovesicles supernatant fluid (P-ELNs SNF) (Figure 1A, top left). The pellet was subjected to repeated washing and resuspension in PBS, followed by transfer into a sucrose gradient (8%/30%/45%/60%) and further centrifugation at 150,000 ×*g* for 120 minutes. Bands between the 8%/30% and 30%/45% layers were harvested, designated as P-ELNs1 and P-ELNs2, respectively. The protein concentration of P-ELNs was quantified using the BCA assay kit (Beyotime, China).

Characterization of P-ELNs

For the characterization of P-ELNs, P-ELNs1, and P-ELNs2, their size and morphology were analyzed using Transmission Electron Microscopy (TEM) (HT7700, Hitachi, Japan). A 20 μL aliquot of the P-ELNs sample was placed on a carbon-coated copper grid for 3–5 minutes. Excess liquid was then carefully removed with filter paper. Subsequently, 2% phosphotungstic acid was applied to the grid for 1–2 minutes, followed again by the removal of excess liquid with filter paper and drying at room temperature. The samples were then observed under TEM, and images were obtained for analysis.

The ζ potential of each particle was measured using a Nanocolter counter (Resun-G02, Resun Technology, China). During the experiments, a nanometer pore chip with a measurement range of 60–200 nm was selected.

Particle size distribution was determined using a Nanoparticle Tracking Analysis (NTA) instrument (Zetasizer Nano ZS, Malvern Panalytical, UK).

Principal Component Analysis of P-ELNs

RNA extraction from P-ELNs was performed using the phenol-chloroform method (9109, TaKaRa, Japan), and the RNA concentration was determined. The extracted P-ELNs RNA was divided into two aliquots. One aliquot remained untreated and served as a control. The other aliquot was incubated with ribonuclease (10 μg/mL) at 37°C for 30 minutes. For analysis, 10 μL of each sample was loaded onto a 2.5% agarose gel for electrophoresis, followed by UV visualization.

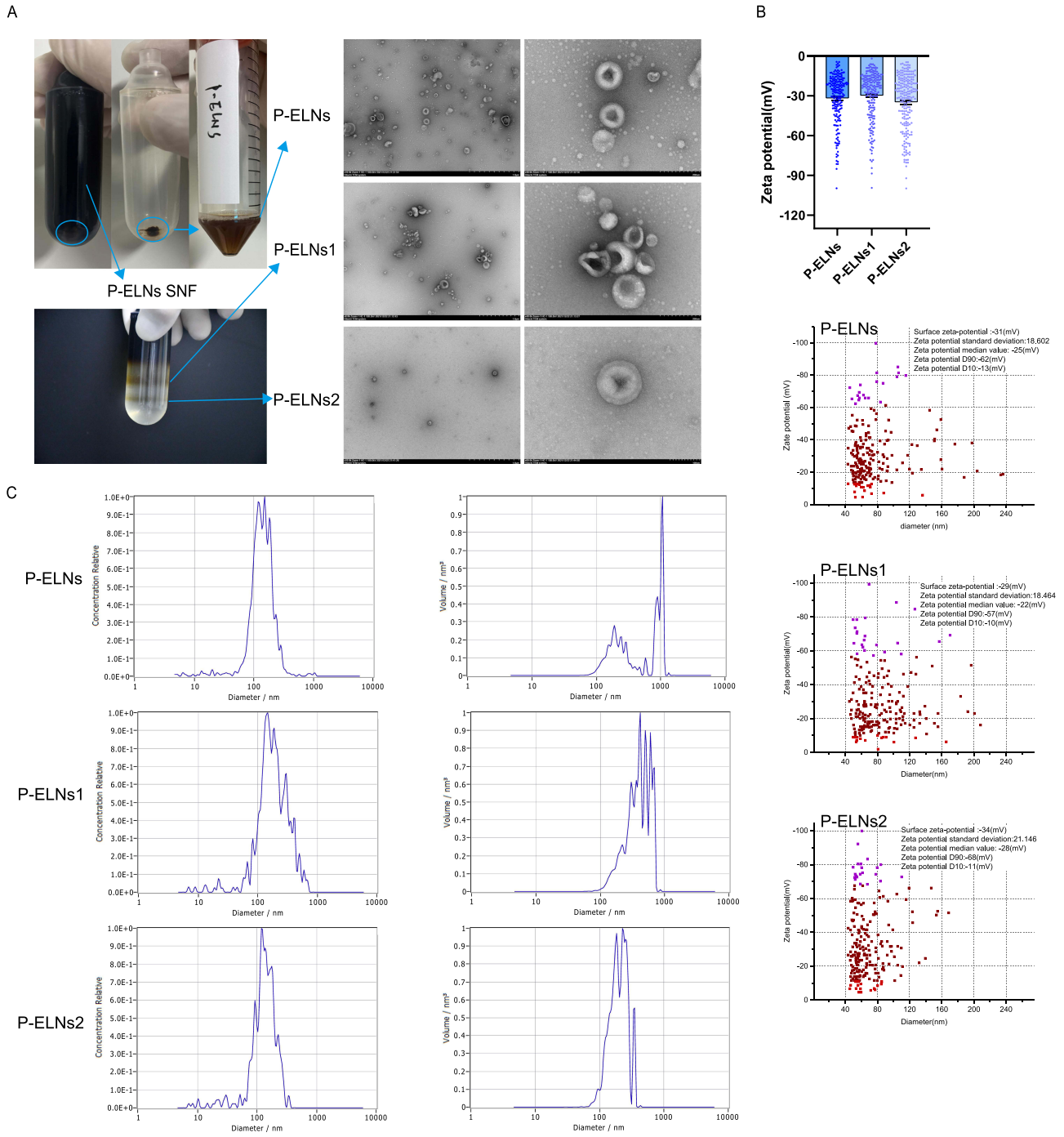

Figure 1 Characterization of P-ELNs, P-ELNs1, and P-ELNs2, Extract photos ((**A**), left), TEM images ((**A**), right), ζ potential (**B**), and NTA (**C**). TEM images include scale bars of 1 μm and 200 nm.

Abbreviations: NTA, nanoparticle tracking analysis; TEM, transmission electron microscopy; P-ELNs, *Pueraria lobata* root - exosome-like nanovesicles.

To extract proteins from P-ELNs, a lysis buffer containing RIPA, PMSF, NaF, and Na3VO3 in the ratio of 100:1:1:1 was used. 10 μL of the protein extract was then loaded onto an SDS-PAGE gel, and the proteins were visualized using Coomassie Brilliant Blue staining.

Lipids were purified from P-ELNs using the Folch method. The lipids were then separated on a silica gel Thin-Layer Chromatography (TLC) plate (HX29848329, Millipore, Germany) using a solvent mixture of chloroform/methanol/acetic acid (9:4:0.5, v/v) as the developing agent. Visualization was conducted under UV light.

Experimental Animals

In the described experiments, female C57BL/6J mice aged 10 weeks (20–22g) and male C57BL/6J mice aged 8 weeks (20–22g) were procured from Sepharose (Beijing) Biotech Co., Ltd. During the acclimation period, the mice were provided with a standard diet supplied by Jiangsu Xietong Pharmaceutical Bio-engineering Co., Ltd.

Optimal Concentration Determination Experiment for P-ELNs

Male C57BL/6J mice were randomly divided into five groups, each consisting of 15 mice. The groups were: Normal Control (NC), PBS + Ethanol (EtOH), 2 mg/(kg.bw) P-ELNs + EtOH, 10 mg/(kg.bw) P-ELNs + EtOH, and 50 mg/(kg.bw) P-ELNs + EtOH. All mice were fasted for 12 hours prior to the experiment. Each group was administered a single dose of their respective treatments (the NC group received PBS by gavage). After 30 minutes, all groups except the NC were administered 15.625mL/(kg.bw) of 40% ethanol (analytical grade, diluted with distilled water, Chongqing Chuandong Chemical Co., LTD.) by gavage [equivalent to an ethanol dose of 5g/(kg.bw)] to induce the model. After alcohol administration via gavage, mice were anesthetized with pentobarbital sodium at 60, 120, and 240 minutes post-gavage, followed by euthanasia for sample collection (n=5).

Intoxication Experiment

In a randomized controlled experiment, 45 male and 45 female C57BL/6J mice (15 per group) received varying ethanol doses (3.6, 5.0, or 6.4 g/(kg.bw), 40% volume fraction, following a 12-hour fast. The onset and proportion of ethanol intoxication (measured by Loss of Righting Reflex (LORR) within less than 5 minutes, 5–10 minutes, and more than 10 minutes) were assessed.

Note: The intoxicated mice were not euthanized, and they were kept for a period of time before being used for other preliminary experiments or model construction.

Acute Alcoholism Experiment (AAI)

C57BL/6J mice were randomly divided into four groups: NC, PBS + EtOH, P-ELNs SNF + EtOH, and P-ELNs + EtOH. All groups were fasted for 12 hours before the experiment and were then given a single dose of their respective treatments (NC group received PBS by gavage). After 30 minutes, all groups except the NC were administered ethanol (40% volume fraction) to induce the model. The dosage for male mice (6 per group) was 15.625 mL/(kg.bw), and for female mice (6 per group), it was 20 mL/(kg.bw) [equivalent to an ethanol dose of 6.4g/(kg.bw)]. The Ebriety time (Time to LORR, the time from consciousness to loss of righting reflex) was observed and recorded. Ebriety was determined based on the disappearance of the righting reflex: after ethanol administration, mice were placed on their backs in the cage, and those maintaining this position for over 30 seconds were considered intoxicated. The Sober-up time (LORR duration, the duration required for recovery from ethanol-induced unconsciousness and ataxia) was also recorded.[27] Mice were euthanized using pentobarbital sodium anesthesia within 6–10 hours after alcohol administration, followed by subsequent tissue collection.

Biochemical Marker Detection

The concentration of various components such as ethanol, alcohol dehydrogenase (ADH), acetaldehyde dehydrogenase (ALDH), and reduced glutathione (GSH) were measured using specific assay kits. The kits used include the ethanol assay kit (Y1D, Cominbio, China), ADH assay kit (ADH1W, Cominbio, China), ALDH assay kit (ALDH, Cominbio, China), and GSH assay kit (BC1175, Solarbio, China). These kits facilitate the quantitative determination of these biochemical markers in the samples.

Western Blot (WB) Analysis

For Western blotting, samples stored in liquid nitrogen were thawed and lysed with RIPA lysis buffer (P0013B, Beyotime, China) to extract proteins. The proteins were then separated by conventional SDS-PAGE (PG112, Epizyme, China) and transferred onto a PVDF membrane (IPVH00010, Millipore, US). The membrane was blocked using a rapid blocking solution (12,010,020, Bio-Rad, US) and incubated overnight with primary antibodies. HRP-conjugated secondary antibodies were then used for immunoblotting. Protein signals were detected using a multifunctional imaging system (UVP Chemstudio touch, Jena, Germany). Quantitative analysis of the protein bands was performed using Image J software.

Oil Red O Staining

Liver frozen sections prepared with a cryostat (CRYOSTAR NX50, Thermo, US) were equilibrated to room temperature before being fixed for 15 minutes using a tissue fixative solution (G1101, Servicebio, China). After a thorough rinsing with tap water and air-drying, the sections were immersed in Oil Red O working stain (G1015, Servicebio, China) for 8–10 minutes, with emphasis placed on covering to shield from light. A brief differentiation was then carried out in two 60% isopropanol baths, followed by rinsing in two distilled water baths. Post-rinsing, the sections were counterstained with hematoxylin (G1004, Servicebio, China) for 3–5 minutes and washed three to five times with pure water. This was followed by a brief differentiation in the differentiation solution and two subsequent pure water rinses to "blue" the sections. The staining quality was assessed under a microscope, after which the sections were mounted using a glycerol gelatin mounting medium. Finally, microscopic examination and image capture were conducted for analytical purposes.

Statistical Analysis and Data Processing

The data presented in this study were analyzed using GraphPad Prism software, version 8.0 (GraphPad Software, Inc., USA). The statistical analysis was conducted using one-way or two-way ANOVA, followed by post hoc multiple comparisons performed with Tukey's and Dunnett's tests. Graphical representations were generated using the same software. These experiments were replicated a minimum of three times to ensure reliability.

Results were expressed as the mean ± SEM. Significance levels in the figures were denoted as $p < 0.05$. Any deviations or additional annotations provided in the text supersede these general criteria. This approach ensures that the statistical analysis is both rigorous and transparent, allowing for the accurate interpretation of the experimental data.

Results

Characterization of P-ELNs

Fresh *P. lobata* roots were utilized to extract and isolate natural exosome-like vesicles (P-ELNs) via differential centrifugation. This was followed by a sucrose density gradient ultracentrifugation refinement step, which concentrated the P-ELNs at specific interfaces within the gradient (Figure 1A, left). Advanced techniques like TEM (Figure 1A, right), Nanocolter ζ potential meter (Figure 1B), and Zetasizer Nano ZS NTA instrument (Figure 1C) were employed to assess the vesicles' integrity, charge, and size. The results revealed that the P-ELNs were nanometric, with diameters of 150.7 ± 82.8 nm, 209.7 ± 118.4 nm, and 142.1 ± 58.1 nm for the isolated P-ELNs, P-ELNs1, and P-ELNs2, respectively. The ζ potential values were consistently negative, concentrated around −31 mV, −29 mV, and −34 mV, respectively, indicating the characteristic structure of exosome vesicles. Subsequent research focused on evaluating the role of P-ELNs in mice exposed to alcohol.

Principal Component Analysis of P-ELNs

In the context of the principal component analysis of P-ELNs, standard purification methods were employed to extract proteins, RNA, and lipids. Upon separation on SDS-polyacrylamide gels and visualization with Coomassie staining, a spectrum of protein bands was revealed (Figure 2B). BCA assays quantified P-ELN protein concentrations at 5.28 ± 0.05, 4.31 ± 0.04, and 0.68 ± 0.04 mg/mL for P-ELNs, P-ELNs1, and P-ELNs2, respectively (Figure 2A). P-ELNs primarily contained small, RNase-sensitive RNA species (Figure 2C). TLC analysis confirmed the presence of diverse lipids within P-ELNs, while puerarin (a flavonoid) was scarce in P-ELNs but abundant in the P-ELNs Supernatant Fluid (SNF) (Figure 2D). These findings collectively demonstrate that P-ELNs possess characteristics consistent with plant-derived exosomal content.

Optimal Concentration Determination of Pre-Oral Administration of P-ELNs in Ethanol-Exposed Mice

It is now understood that during the hepatic metabolism of ethanol within the physiological context, two enzymatically catalyzed reactions play a central role. Initially, alcohol dehydrogenase 1 (ADH1) facilitates the oxidation of most of the ethanol to acetaldehyde. Subsequently, aldehyde dehydrogenase 2 (ALDH2) and its cofactors further oxidize acetaldehyde to acetic acid primarily within the mitochondria, while a minor portion undergoes oxidation in the cytoplasm by ALDH1 and its cofactors.[5] A critical aspect in determining the most effective concentration of orally administered P-ELNs in ethanol-exposed

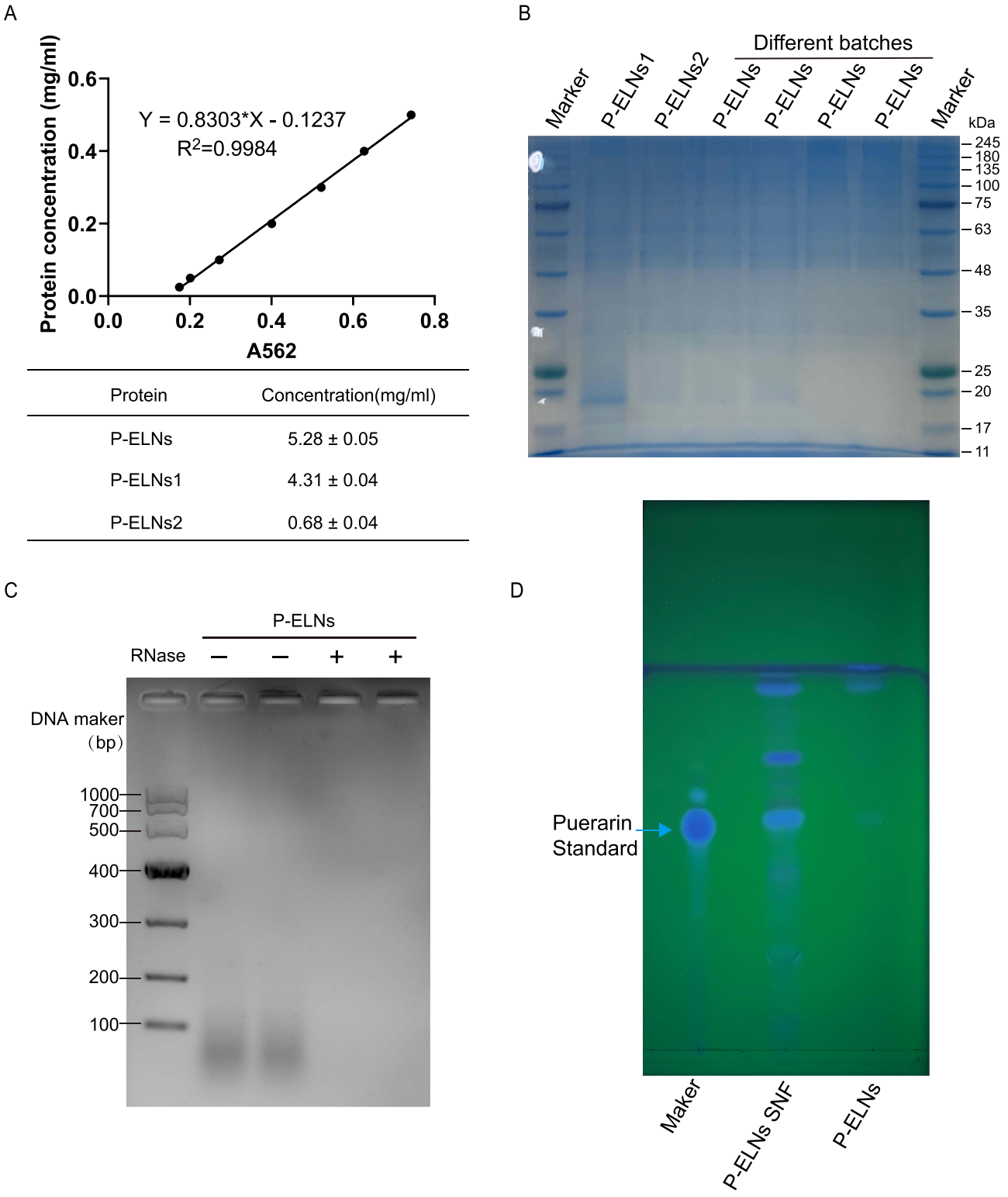

Protein	Concentration(mg/ml)
P-ELNs	5.28 ± 0.05
P-ELNs1	4.31 ± 0.04
P-ELNs2	0.68 ± 0.04

Figure 2 Analysis of the principal components of P-ELNs via protein BCA assay (**A**), Coomassie staining (**B**), RNA agarose gel (**C**), and TLC (**D**).
Abbreviation: TLC, lipid thin-layer chromatography.

mice involves investigating hepatic alcohol metabolism, including liver ALDH and ADH activities, as well as serum ethanol concentration. Through assessments of liver ALDH and ADH activities, along with serum EtOH levels, it was observed that a concentration of 10 mg/kg.bw P-ELNs significantly reduced hepatic alcohol concentration ($p<0.05$, Figure 3B), markedly

enhanced hepatic ALDH activity ($p<0.05$, Figure 3C), and the administration of P-ELNs at a dosage of 50 mg/kg body weight was found to be the most effective in reducing liver ADH activity ($p<0.05$, Figure 3D). Although variations in serum ethanol concentrations across groups were not statistically significant, the 10 mg/kg.bw P-ELNs group exhibited a p-value of 0.0519 compared to the model group (Figure 3A). This lack of significant difference can be attributed to two factors: firstly, the time required for the transport of metabolized alcohol from the liver to the bloodstream; secondly, the relatively small number of mice sampled at each time point in the experiment (n=5). Therefore, an integrated analysis concludes that 10 mg/kg.bw P-ELNs represents the optimal dose for improving alcohol metabolism.

Effect of Oral Administration of P-ELNs on the Righting Reflex in Mice with AAI

The requirement for the mice righting reflex experiment is that mice can rapidly become intoxicated, and their time to loss of righting reflex, referred to as "Ebriety time" (Time to LORR), and the number of mice exhibiting signs of intoxication was meticulously recorded. Due to variations in gender-specific drinking patterns among humans, we conducted a study to quantify the differential alcohol consumption between male and female mice during a specific timeframe of intoxication. When male mice were administered ethanol at a concentration of 5.0 g/(kg.bw) [40% ethanol by volume, administered at 15.625 mL/(kg.bw)], the proportion of intoxication within 5–10 minutes was 66.67% (Figure 4A). In contrast, for female mice

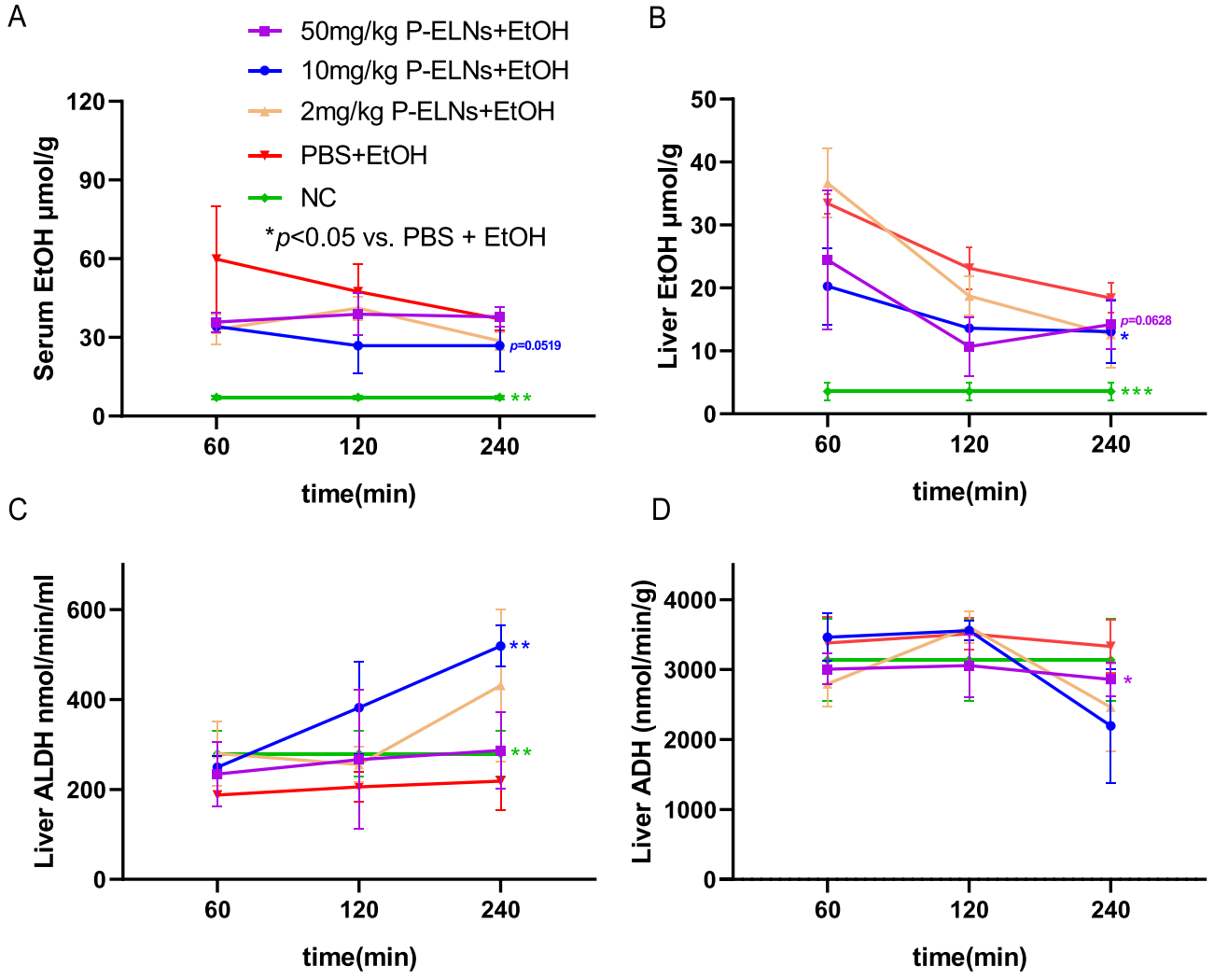

Figure 3 Evaluation of the optimal pre-oral dose of P-ELNs (0 [PBS], 2, 10, and 50 mg/(kg.bw)) in ethanol-exposed mice. Post-alcohol gavage, samples were collected at 60, 120, and 240 minutes for serum (**A**) and hepatic alcohol content (**B**), as well as hepatic ALDH (**C**) and ADH enzyme activity (**D**) analysis (n=5, *$p<0.05$, **$p<0.01$, ***$p<0.001$ vs PBS + EtOH).

Abbreviations: ADH, alcohol dehydrogenase; ALDH, acetaldehyde dehydrogenase.

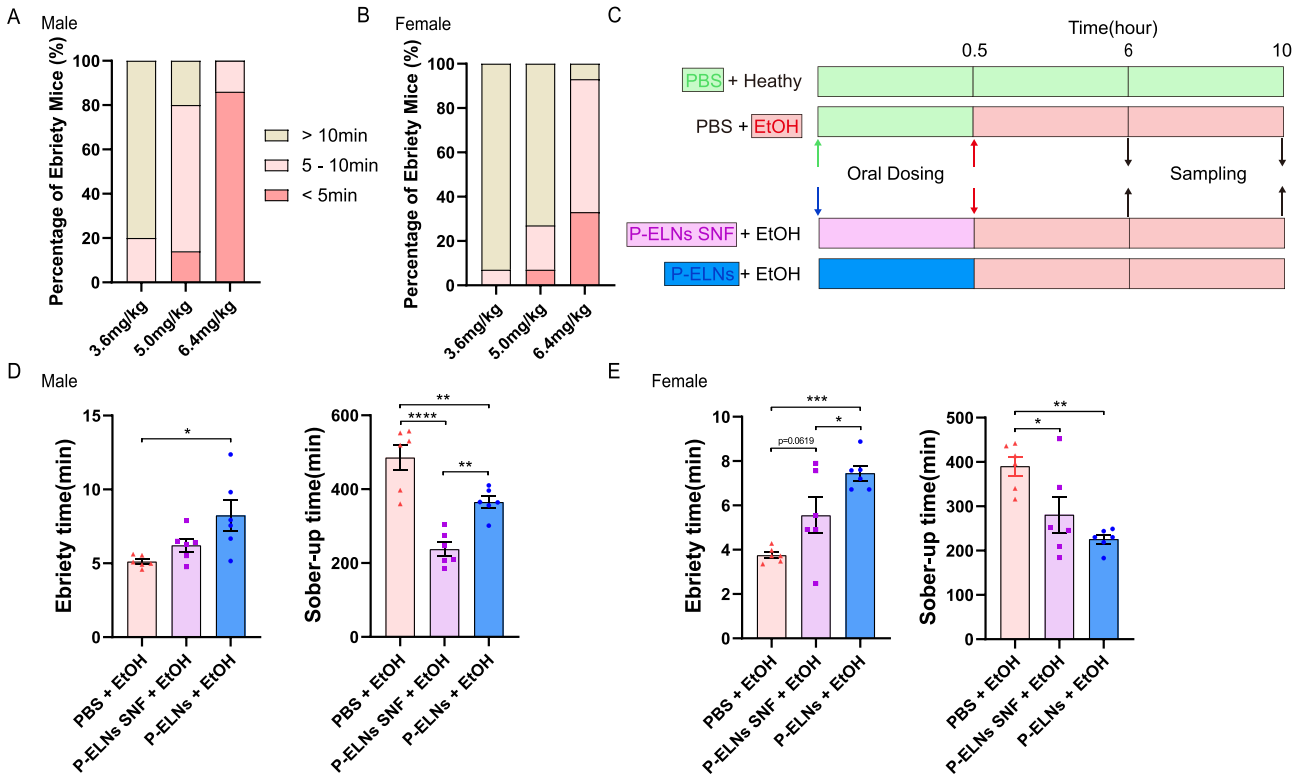

Figure 4 Percentage of intoxicated mice following varying alcohol doses (3.6, 5.0, and 6.4 g/(kg.bw)) over different time intervals (<5, 5–10, and >10 min) in male and female mice (male in (**A**), female in (**B**), n=15); A schematic diagram of the P-ELNs oral administration in the AAI mice model (**C**) and the LORR experiment of the Ebriety and Sober-up time in AAI mice after oral administration of P-ELNs (male in (**D**), female in (**E**), n=6, *p<0.05, **p<0.01, ***p<0.001, ****p<0.0001).
Abbreviations: AAI, acute alcoholism; LORR, loss of righting reflex.

to reach a 60% intoxication rate within 5–10 minutes, the required ethanol concentration was 6.4 g/(kg.bw) [40% ethanol by volume, administered at 20 mL/(kg.bw)] (Figure 4B). Conversely, epidemiological studies have indicated that women exhibit a higher susceptibility to alcohol-induced liver damage compared to men.[28] This vulnerability can be attributed to factors such as lower body weight and higher body fat content in women, which ultimately contribute to the manifestation of more pronounced alcohol-related liver damage. However, in *Sprague-Dawley* or *Wistar* rats of consistent weight, there is no significant difference in susceptibility to liver damage induced by ethanol.[29] Based on these observations, we infer that the differences in our intoxication experiment results may be due to age in weeks, hormonal levels, alcohol metabolism-related enzyme activities, and pharmacokinetics in male and female C57 mice of similar weight (8-week-old male and 10-week-old female). The more rapid and pronounced ethanol metabolism in female mice might be attributable to these factors. Consequently, considering these reasons and the gender differences involved in human alcohol consumption, our subsequent experiments will be conducted separately in male and female mice to observe and study the differences in alcohol metabolism after the oral administration of P-ELNs in ethanol-exposed mice.

Building upon the preceding experimental findings, the Loss of Righting Reflex experiment was executed according to the AAI animal model schematic (Figure 4C). In the righting reflex experiment involving male mice, pre-oral administration of P-ELNs significantly increased Ebriety time (time to LORR, p<0.05) and reduced Sober-up time (duration of LORR, p<0.05) (Figure 4D), displaying more efficacy compared to P-ELNs SNF. Similar outcomes were observed in high-dose alcohol-exposed female mice (Figure 4E), where the effects were more pronounced than those of P-ELNs SNF. Intriguingly, in high-dose alcohol-exposed female mice, oral administration of P-ELNs proved more effective in shortening Sober-up time, while P-ELNs SNF exhibited a diminishing effect on reducing Sober-up time as the alcohol concentration increased (from male to female mice). This observation may also be linked to gender differences in alcohol tolerance among mice.

Biochemical Markers of Alcohol Metabolism in Mice with AAI

In the setting of AAI, the duration of intoxication and recovery in mice displaying a loss of righting reflex serves as the most direct phenotypic indicator of intoxication. Meanwhile, biochemical markers of alcohol metabolism provide substantial evidence of the organism's response to alcohol exposure. In the righting reflex experiment involving male C57 mice pre-orally administered with P-ELNs, a significant decrease in both ADH activity and serum ethanol concentration ($p<0.05$) (Figure 5A) was observed, surpassing the results from mice administered with P-ELNs SNF. Similarly, in the experiment with female mice exposed to higher alcohol doses, pre-oral administration of P-ELNs significantly increased hepatic ALDH activity ($p<0.05$) and decreased ADH activity ($p<0.05$), although the reduction in serum alcohol content was not substantial (Figure 5B). This effect also surpassed that of P-ELNs SNF administration. The observed differences between male and female C57 mice are presumed to be inherently linked to variations in alcohol exposure dosages and gender-specific physiological differences.

Furthermore, an intriguing observation was made. Traditionally, the alcohol detoxification and liver-protective effects of *P. lobata* have been attributed to puerarin, a constituent of the root. However, through principal component analysis of puerarin content (Figure 2D), Ebriety and Sober-up times (Figures 4D and E), as well as biochemical markers (Figure 5), it was demonstrated that the anti-Intoxication and alcohol metabolism-promoting of P-ELNs is not solely due to puerarin but other active components present in P-ELNs.

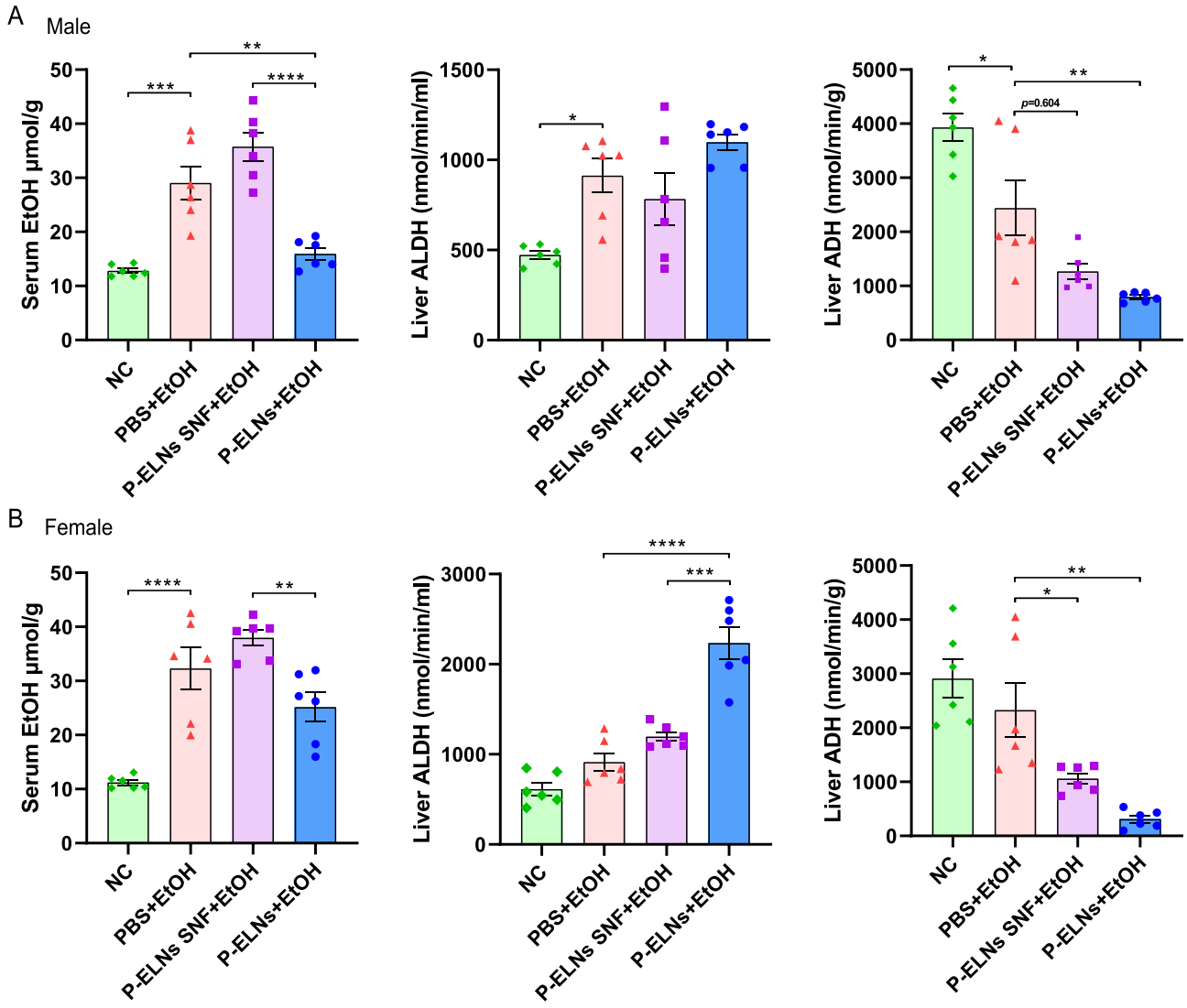

Figure 5 Biochemical markers of alcohol metabolism, including serum alcohol content and hepatic ALDH and ADH enzyme activity (male in (**A**), female in (**B**) in AAI mice by oral administration of P-ELNs (n=6, *$p<0.05$, **$p<0.01$, ***$p<0.001$, ****$p<0.0001$).

P-ELNs Mitigate Alcohol-Induced Ferroptosis in Mice

Subsequently, we assessed the alterations in alcohol metabolism and ferroptosis markers in hepatic cells using liver tissues from mice acutely intoxicated with alcohol and pre-treated with P-ELNs.

It has been established that ADH1, highly expressed in the liver, stomach, kidney, and colon tissues, plays a crucial role in the oxidation of most ethanol in the liver.[5] Besides, cytoplasmic ethanol can induce Cytochrome P450 Family 2 Subfamily E Member 1 (CYP2E1), oxidizing a portion of ethanol to acetaldehyde.[30] ALDH2, the primary isoenzyme catalyzing acetaldehyde conversion, has a Michaelis constant (Km) about one-tenth of that of ALDH1.[5] In the present study, during the righting reflex experiment with male C57 mice, post-P-ELNs treatment led to a significant increase in hepatic ALDH2 and CYP2E1 protein levels ($p<0.05$), while ADH1 levels remained relatively unchanged (Figure 6A). Similarly, in female C57 mice exposed to higher alcohol doses, ALDH2 changes were consistent with those in males ($p<0.05$), but variations in CYP2E1 and ADH1 were not significant (Figure 6B). The abrupt decline in CYP2E1 protein levels from low-dose male to high-dose female mice might be attributed to ethanol serving as a substrate for enzyme-catalyzed reactions, where increased ethanol dosage could lead to threshold limits or feedback inhibition, and possibly to differences in enzymatic activity between genders.

Liver cells, rich in mitochondria, are susceptible to ferroptosis induced by excessive alcohol exposure.[23] GPX4, a pivotal factor resisting ferroptosis, functions by selenium-dependent reduction of lipid peroxides using GSH.[31,32] Excessive lipid peroxidation destabilizes lipid bilayers, leading to cellular membrane disintegration and increased sensitivity to ferroptosis. Acyl-CoA synthetase long-chain family member 4 (ACSL4), a key enzyme regulating lipid composition, promotes ferroptosis, while Ferritin Heavy Chain 1 (FTH1) disrupts iron autophagosomes, inhibiting ferroptosis.[31] In male C57 mice (Figure 6A), compared to healthy males pre-treated with PBS (NC group), those exposed to alcohol post-PBS treatment exhibited a significant reduction in hepatic GPX4 levels ($p<0.05$), consistent with existing literature on alcohol-induced ferroptosis.[22,23] Variations in the intensity of Western Blot (WB) bands indicate that individual differences in male mice contribute to subtle changes in ACSL4 and FTH1 protein levels. In contrast, post-P-ELNs treatment in alcohol-exposed males significantly increased GPX4 ($p<0.05$) and decreased ACSL4 ($p<0.05$), suggesting tolerance or inhibition of ferroptosis and mitigating its occurrence. As ferroptosis involves decreased GPX4 activity and GSH depletion, GSH levels in male C57 mice were measured (Figure 6B), showing no significant differences. Furthermore, we assessed ferroptosis markers in the livers of female mice exposed to higher alcohol concentrations post-P-ELNs treatment (Figure 6C), observing changes in GPX4 levels ($p<0.05$) consistent with male mice, while variations in ACSL4 and FTH1 remained inconspicuous, correlating with individual differences and alcohol metabolism. Liver GSH content analysis (Figure 6D) confirmed the presence of ferroptosis, with a significant rise in GSH levels ($p<0.05$). Lipid peroxidation, a crucial marker of ferroptosis, was evident in Oil Red O staining liver sections of C57 mice (Figure 6E), with pathological changes like extensive hepatocyte lipid droplets and cellular atrophy in alcohol-exposed mice post-PBS treatment. These were substantially inhibited in livers of mice pre-treated with P-ELNs. Hence, the results suggest that P-ELNs appear to inhibit alcohol-induced ferroptosis, preventing hepatic lipid accumulation.

Discussion

P. lobata is a commonly consumed ingredient in daily diets, recognized in Traditional Chinese Medicine for its hepatoprotective properties. Among these, the extract of *P. lobata* - Puerarin (comprising total flavonoids and isoflavones) has exhibited efficacy in studies pertaining to alcohol-induced liver protection.[16,17] This constituent effectively counteracts the central nervous system depression induced by excessive alcohol consumption, reduces sleep duration in mice, and ameliorates acute alcohol poisoning as well as hepatic injury.[18] Furthermore, it also regulates blood hormone levels and free radical concentrations while mitigating blood viscosity.[33] However, the effectiveness of *P. lobata*, both as a dietary component and medicinal agent, is directly proportional to dosage, leading to suboptimal therapeutic effects. Traditional preparation techniques contribute to the loss of active components, with most research focusing on puerarin present in dried *P. lobata* powder. While there are various medications available for liver damage protection, the options for alcohol detoxification and promoting wakefulness are limited, often involving substances with addiction potential and residual effects.[6,7] In this context, our study introduces P-ELNs, distinct exosome-like structures extracted from *P. lobata*.

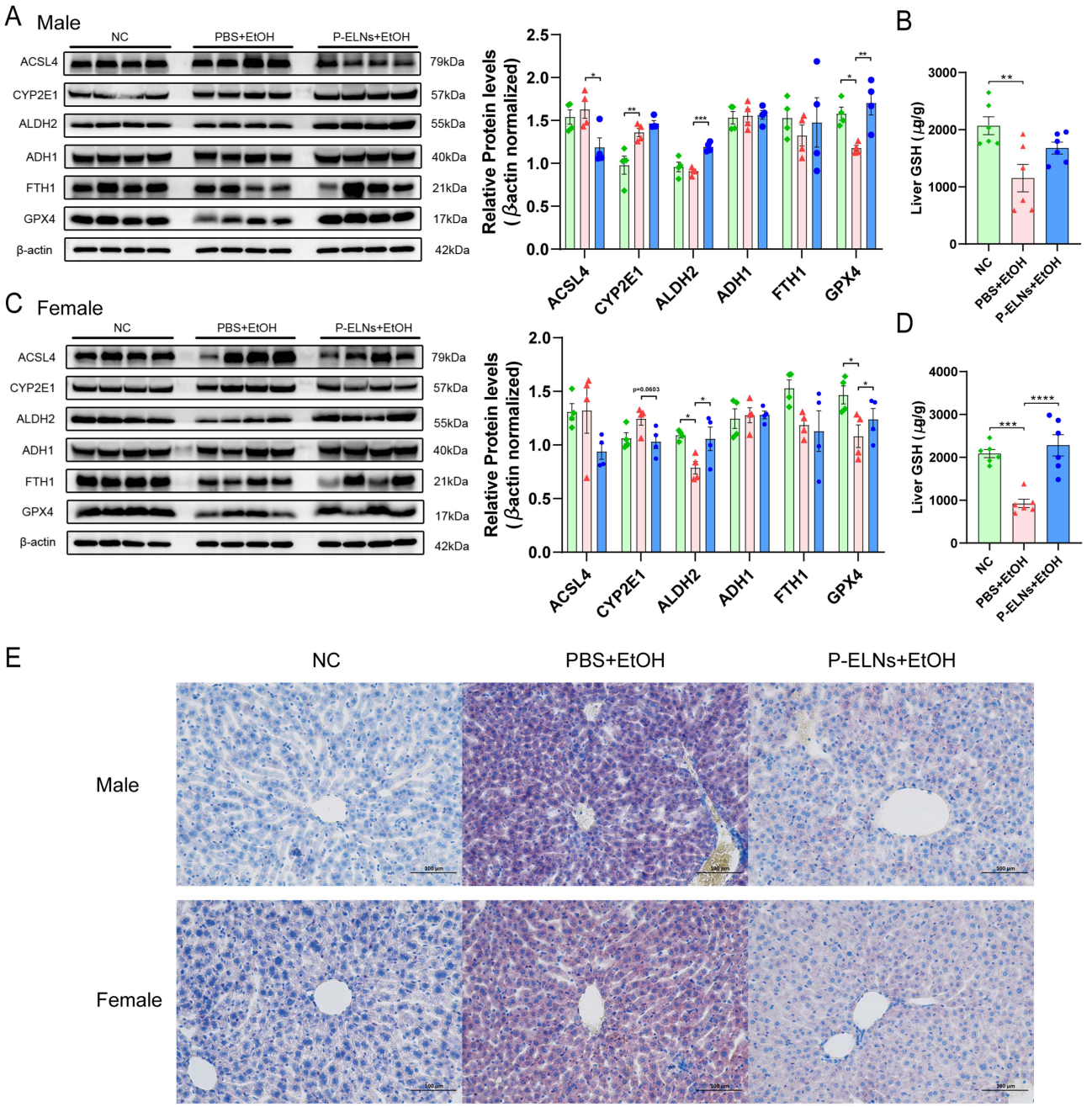

Figure 6 Hepatic alcohol metabolism and ferroptosis protein biomarkers (male in (**A**), n=4), liver GSH content (male in (**B**), n=6), hepatic alcohol metabolism and ferroptosis protein biomarkers (female in (**C**), n=4), liver GSH content (female in (**D**), n=6) and changes in Oil Red O staining (**E**) in AAI mice by oral administration of P-ELNs (*p<0.05, **p<0.01, ***p<0.001, ****p<0.0001).
Abbreviation: GSH, reduced glutathione.

Remarkably, oral administration of 10 mg/(kg.bw) P-ELNs could effectively mitigate the effects of alcohol Intoxication and potentially improve alcohol metabolism in both male and female mice, with female mice showing particularly promising outcomes. Notably, the higher performance of pre-oral administration of P-ELNs compared to P-ELNs SNF in reducing Ebriety times and promoting Sober-up times suggests that the effects are not attributed to puerarin, given the negligible puerarin content in P-ELNs and its abundance in P-ELNs SNF as shown in lipid TLC. Next, the active components within P-ELNs will be a focal point for future research, contributing to new possibilities in the realm of alcohol detoxification promotion.

It is now understood that the primary pathway for ethanol metabolism in the liver involves a sequential two-step enzymatic process. Initially, ethanol is converted to acetaldehyde by ADH, and subsequently, acetaldehyde is oxidized to acetic acid by ALDH.[5] Acetaldehyde, an intermediate metabolite, possesses high reactivity and exerts significant hepatotoxicity; its accumulation within the body can result in severe hangover symptoms.[34–36] Therefore, eliminating acetaldehyde can effectively alleviate alcohol-induced hangovers and mitigate liver toxicity. For instance, Tiaogan Jiejiu Tongluo Formula, by lowering the activity of ADH and raising the activity of ALDH, accelerates the conversion of acetaldehyde to acetic acid, alleviates the accumulation of large amounts of acetaldehyde and chronic acetaldehyde poisoning, and reduces the chronic liver injury induced by alcohol in SD rats.[37] Besides, certain functional beverages such as soda water and jia duo bao herbal infusion can also mitigate acetaldehyde levels in the body through ADH inhibition and ALDH enhancement, thus alleviating alcohol-induced hangovers in Kunming mice and preventing liver injury.[38] Additionally, Electrolytic hydrogen water (EHW) demonstrates the ability to reduce intracellular acetaldehyde levels, suppress cellular reactive oxygen species (ROS) elevation, and prevent cell death by inhibiting ADH activity while increasing ALDH activity in HepG2 liver cells.[39] In our investigation using an AAI model in mice, oral administration of P-ELNs resulted in a significant reduction in hepatic ADH activity and a notable increase in ALDH activity, indicating the promotion of acetaldehyde metabolism and elimination through regulation of the ADH/ALDH dehydrogenase system, thereby accelerating alcohol metabolism. Further studies are warranted to elucidate the specific biochemical mechanisms underlying these findings.

Alcohol metabolism primarily occurs in hepatocytes within the body. Excessive alcohol metabolism can disrupt lipid homeostasis, leading to an increased production of lipid peroxides. This disturbance results in the destabilization of lipid bilayers and membrane disintegration, impacting cellular sensitivity to ferroptosis and exacerbating lipid accumulation in liver cells.[22,23,30] Previous studies have demonstrated the involvement of ferroptosis in cell death induced by alcohol both in vivo and in vitro.[24–26,40] Our research also observed significant ferroptosis in liver cells of the control model group exposed to alcohol. Although the mechanism by which plant-derived exosomes mediate ferroptosis in the context of alcohol exposure is not fully understood, our study provided hitherto undocumented evidence that mice pre-treated with P-ELNs and then exposed to alcohol exhibited a notable improvement in liver ferroptosis markers compared to the control model group. This improvement included an increase in GPX4 protein levels and GSH activity, coupled with a decrease in ACSL4 protein levels. According to relevant studies, Alda-1, an ALDH2 activator, has demonstrated efficacy in ameliorating gastric mucosal damage and ferroptosis induced by HCl/ethanol in rats.[41] In contrast, ADH transgenic mice exhibited exacerbated ferroptosis development following alcohol stimulation, resulting in significant alcohol-induced cardiac remodeling, functional defects, and insulin resistance.[42] Therefore, we propose that P-ELNs alleviate alcohol-induced liver injury by enhancing the enzyme system associated with alcohol metabolism and inhibiting key components involved in ferroptosis. This finding holds great significance and offers a potential approach for utilizing plant-derived exosomal vesicles as preventive or therapeutic agents against alcohol-related liver injury.

Conclusion

Our study shows that fresh *P. lobata* roots can extract natural exosomal-like nanovesicles, which have obvious plant exosome characteristics. They contain rich biologically active functional molecules and show better biocompatibility and utilization. P-ELNs significantly enhance anti-intoxication and alcohol metabolism potential in the AAI mice. This is different from previous studies, as the observed effects are not due to the action of puerarin found in *P. lobata* roots. The active components of P-ELNs that play a key role, as well as the underlying mechanisms involved, will be the focus of our future research. Furthermore, it has been observed that P-ELNs not only facilitate alcohol metabolism but also exhibit a suppressive effect on the progression of ferroptosis and mitigate acute alcohol-induced liver injury. Considering the current emphasis on investigating the role of P-ELNs in promoting alcohol metabolism and protecting against acute liver injury, further comprehensive exploration is warranted to elucidate their protective effects on chronic liver injury. In summary, this study provides initial insights into the anti-intoxication and alcohol metabolism-promoting effects of P-ELNs and their related mechanisms, which lays theoretical foundation for the development of novel health agents for alcohol detoxification and liver protection in the future.

Ethics Approval

All animal experiments were conducted in accordance with the guidelines and regulations set forth by the Animal Ethics Committee of the Chongqing University Three Gorges Hospital (IACUC approval number: SXYYWD2023-001) and performed under the supervision of trained professionals certified by the Chongqing Technical Association (certificate numbers: CQLA-2023-0052, CQLA-2023-0053).

Acknowledgments

We extend our profound gratitude to all authors for their participation and contributions to this study. This research was supported by the Chongqing Municipality Clinical Research Center for Endocrinology and Metabolic Diseases Construction Fund (No. 66002) and the Chongqing medical scientific research project (Joint project of Chongqing Health Commission and Science and Technology Bureau) (grant number: 2024QNXM054). These grants have been instrumental in facilitating the research, providing essential resources and funding necessary to achieve the study's objectives.

Disclosure

All authors report the patent "A pueraria-derived exosome-like nanoparticle: preparation, characterization, and potential applications" was issued by the State Intellectual Property Office of China to Chongqing University Three Gorges Hospital. The authors report no other conflicts of interest in this work.

References

1. World Health O. Global status report on alcohol and health 2018. Geneva: World Health Organization; 2018. Available from: https://iris.who.int/handle/10665/274603. Accessed May 24, 2024.
2. Manthey J, Shield KD, Rylett M, Hasan OSM, Probst C, Rehm J. Global alcohol exposure between 1990 and 2017 and forecasts until 2030: a modelling study. *Lancet*. 2019;393(10190):2493–2502. doi:10.1016/S0140-6736(18)32744-2
3. Seitz HK, Bataller R, Cortez-Pinto H, et al. Alcoholic liver disease. *Nature Reviews Disease Primers*. 2018;4(1):7. doi:10.1038/s41572-018-0014-7
4. Singal AK, Bataller R, Ahn J, Kamath PS, Shah VH. ACG Clinical Guideline: alcoholic Liver Disease. *Am J Gastroenterol*. 2018;113(2):175–194. doi:10.1038/ajg.2017.469
5. Louvet A, Mathurin P. Alcoholic liver disease: mechanisms of injury and targeted treatment. *Nat Rev Gastroenterol Hepatol*. 2015;12(4):231–242. doi:10.1038/nrgastro.2015.35
6. Modesto-Lowe V, Fritz EM. The opioidergic-alcohol link: implications for treatment. *CNS Drugs*. 2005;19(8):693–707. doi:10.2165/00023210-200519080-00005
7. Liang J, Olsen RW. Alcohol use disorders and current pharmacological therapies: the role of GABAA receptors. *Acta Pharmacol. Sin.* 2014;35(8):981–993. doi:10.1038/aps.2014.50
8. Yanez-Mo M, Siljander PR, Andreu Z, et al. Biological properties of extracellular vesicles and their physiological functions. *J Extracell Vesicles*. 2015;4:27066. doi:10.3402/jev.v4.27066
9. Yoshioka Y, Konishi Y, Kosaka N, Katsuda T, Kato T, Ochiya T. Comparative marker analysis of extracellular vesicles in different human cancer types. *J Extracell Vesicles*. 2013;2. doi:10.3402/jev.v4.27066
10. Théry C, Witwer KW, Aikawa E, et al. Minimal information for studies of extracellular vesicles 2018 (MISEV2018): a position statement of the International Society for Extracellular Vesicles and update of the MISEV2014 guidelines. *J Extracell Vesicles*. 2018;7(1). doi:10.1080/20013078.2018.1535750
11. Subudhi PD, Bihari C, Sarin SK, Baweja S. Emerging Role of Edible Exosomes-Like Nanoparticles (ELNs) as Hepatoprotective Agents. *Nanotheranostics*. 2022;6(4):365–375. doi:10.7150/ntno.70999
12. Zhuang X, Deng ZB, Mu J, et al. Ginger-derived nanoparticles protect against alcohol-induced liver damage. *J Extracell Vesicles*. 2015;4:28713. doi:10.3402/jev.v4.28713
13. Liu B, Lu Y, Chen X, et al. Protective Role of Shiitake Mushroom-Derived Exosome-Like Nanoparticles in D-Galactosamine and Lipopolysaccharide-Induced Acute Liver Injury in Mice. *Nutrients*. 2020;12(2). doi:10.3402/jev.v4.28713
14. Kim J-S, Kim D-H, Gil M-C, et al. Pomegranate-Derived Exosome-Like Nanovesicles Alleviate Binge Alcohol-Induced Leaky Gut and Liver Injury. *Journal of Medicinal Food*. 2023;26(10):739–748. doi:10.1089/jmf.2023.K.0060
15. Xu F, Mu J, Teng Y, et al. Restoring Oat Nanoparticles Mediated Brain Memory Function of Mice Fed Alcohol by Sorting Inflammatory Dectin-1 Complex Into Microglial Exosomes. *Small*. 2022;18(6):e2105385. doi:10.1089/jmf.2023.K.0060
16. Zhou YX, Zhang H, Peng C. Puerarin: a review of pharmacological effects. *Phytother Res*. 2014;28(7):961–975. doi:10.1002/ptr.5083
17. Liu YS, Yuan MH, Zhang CY, et al. Puerariae Lobatae radix flavonoids and puerarin alleviate alcoholic liver injury in zebrafish by regulating alcohol and lipid metabolism. *Biomed Pharmacother*. 2021;134:111121. doi:10.1016/j.biopha.2020.111121
18. Zhang Z, Li S, Jiang J, Yu P, Liang J, Wang Y. Preventive effects of Flos Perariae (Gehua) water extract and its active ingredient puerarin in rodent alcoholism models. *ChinMed*. 2010;5(1). doi:10.1186/1749-8546-5-36
19. Chen X, Liu B, Li X, et al. Identification of anti-inflammatory vesicle-like nanoparticles in honey. *J Extracell Vesicles*. 2021;10(4):e12069. doi:10.1002/jev2.12069

20. Teng Y, Ren Y, Sayed M, et al. Plant-Derived Exosomal MicroRNAs Shape the Gut Microbiota. *Cell Host Microbe*. 2018;24(5):637–652 e638. doi:10.1016/j.chom.2018.10.001
21. Zu M, Xie D, Canup BSB, et al. 'Green' nanotherapeutics from tea leaves for orally targeted prevention and alleviation of colon diseases. *Biomaterials*. 2021;279:121178. doi:10.1016/j.biomaterials.2021.121178
22. Li LX, Guo FF, Liu H, Zeng T. Iron overload in alcoholic liver disease: underlying mechanisms, detrimental effects, and potential therapeutic targets. *Cell Mol Life Sci*. 2022;79(4):201. doi:10.1007/s00018-022-04239-9
23. Shi JF, Liu Y, Wang Y, Gao R, Wang Y, Liu J. Targeting ferroptosis, a novel programmed cell death, for the potential of alcohol-related liver disease therapy. *Front Pharmacol*. 2023;14:1194343. doi:10.3389/fphar.2023.1194343
24. Luo J, Song G, Chen N, et al. Ferroptosis contributes to ethanol-induced hepatic cell death via labile iron accumulation and GPx4 inactivation. *Cell Death Discov*. 2023;9(1):311. doi:10.1038/s41420-023-01608-6
25. Liu CY, Wang M, Yu HM, et al. Ferroptosis is involved in alcohol-induced cell death in vivo and in vitro. *Biosci Biotechnol Biochem*. 2020;84(8):1621–1628. doi:10.1080/09168451.2020.1763155
26. Gao Z, Wang D, Zhang H, et al. An iron-deficient diet prevents alcohol- or diethylnitrosamine-induced acute hepatotoxicity in mice by inhibiting ferroptosis. *Curr Res Food Sci*. 2022;5:2171–2177. doi:10.1016/j.crfs.2022.11.001
27. Choi M, Schneeberger M, Fan W, et al. FGF21 counteracts alcohol intoxication by activating the noradrenergic nervous system. *Cell Metab*. 2023;35(3):429–437.e425. doi:10.1016/j.cmet.2023.02.005
28. Wilsnack RW, Wilsnack SC, Kristjanson AF, Vogeltanz-Holm ND, Gmel G. Gender and alcohol consumption: patterns from the multinational GENACIS project. *Addiction*. 2009;104(9):1487–1500. doi:10.1111/j.1360-0443.2009.02696.x
29. Ronis MJJ, Korourian S, Yoon S, et al. Lack of sexual dimorphism in alcohol-induced liver damage (ALD) in rats treated chronically with ethanol-containing low carbohydrate diets: the role of ethanol metabolism and endotoxin. *Life Sci*. 2004;75(4):469–483. doi:10.1016/j.lfs.2004.01.012
30. Lu Y, Cederbaum AI. CYP2E1 and oxidative liver injury by alcohol. *Free Radic Biol Med*. 2008;44(5):723–738. doi:10.1016/j.freeradbiomed.2007.11.004
31. Tang D, Chen X, Kang R, Kroemer G. Ferroptosis: molecular mechanisms and health implications. *Cell Res*. 2020;31(2):107–125. doi:10.1038/s41422-020-00441-1
32. Ursini F, Maiorino M. Lipid peroxidation and ferroptosis: the role of GSH and GPx4. *Free Radic Biol Med*. 2020;152:175–185. doi:10.1016/j.freeradbiomed.2020.02.027
33. Zhao M, Du Y-Q, Yuan L, Wang -N-N. Protective Effect of Puerarin on Acute Alcoholic Liver Injury. *Am J Chin Med*. 2012;38(02):241–249. doi:10.1142/S0192415X10007816
34. Mello T, Ceni E, Surrenti C, Galli A. Alcohol induced hepatic fibrosis: role of acetaldehyde. *Mol Aspect Med*. 2008;29(1–2):17–21. doi:10.1016/j.mam.2007.10.001
35. Farfán Labonne BE, Gutiérrez M, Gómez-Quiroz LE, et al. Acetaldehyde-induced mitochondrial dysfunction sensitizes hepatocytes to oxidative damage. *Cell Biol Toxicol*. 2009;25(6):599–609. doi:10.1007/s10565-008-9115-5
36. Choe H, Yun I, Kim Y, et al. Effect of herbal extracts and supplement mixture on alcohol metabolism in Sprague Dawley-rats. *J Food Sci Technol*. 2022;59(12):4915–4923. doi:10.1007/s13197-022-05580-4
37. Fang C, Zhang J, Han J, et al. Tiaogan Jiejiu Tongluo Formula attenuated alcohol-induced chronic liver injury by regulating lipid metabolism in rats. *J Ethnopharmacol*. 2023:317. doi:10.1016/j.jep.2023.116838
38. Wang F, Zhang Y-J, Zhou Y, et al. Effects of Beverages on Alcohol Metabolism: potential Health Benefits and Harmful Impacts. *Int J Mol Sci*. 2016;17(3):354. doi:10.3390/ijms17030354
39. Yano S, Wang J, Kabayama S, Hara T. Electrolyzed Hydrogen Water Protects against Ethanol-Induced Cytotoxicity by Regulating Aldehyde Metabolism-Associated Enzymes in the Hepatic Cell Line HepG2. *Antioxidants*. 2021;10(5):801. doi:10.3390/antiox10050801
40. Ding S, Jiang J, Zhang G, Yu M, Zheng Y. Ambient particulate matter exposure plus chronic ethanol ingestion exacerbates hepatic fibrosis by triggering the mitochondrial ROS-ferroptosis signaling pathway in mice. *Ecotoxicol Environ Saf*. 2023;256. doi:10.1016/j.ecoenv.2023.114897
41. Zhang Y, Yuan Z, Chai J, et al. ALDH2 ameliorates ethanol-induced gastric ulcer through suppressing NLPR3 inflammasome activation and ferroptosis. *Arch. Biochem. Biophys*. 2023:743. doi:10.1016/j.abb.2023.109621
42. Lu Q, Qin X, Chen C, et al. Elevated levels of alcohol dehydrogenase aggravate ethanol-evoked cardiac remodeling and contractile anomalies through FKBP5-yap-mediated regulation of ferroptosis and ER stress. *Life Sci*. 2024:343. doi:10.1016/j.lfs.2024.122508